Coordination Chemistry Reviews, 65 (1985) 87–113
Elsevier Science Publishers B.V., Amsterdam – Printed in The Netherlands

RECENT DEVELOPMENTS IN THE STUDIES OF TITANIUM AND VANADIUM PORPHYRINS WITH A SPECIAL EMPHASIS ON OXYGEN ADDUCTS, LOW VALENT METALLOPORPHYRINS, AND RELATED SYSTEMS WITH SULFUR AND SELENIUM

R. GUILARD

Laboratoire de Synthèse et d'Electrosynthèse Organométallique associé au C.N.R.S. (LA 33), Faculté des Sciences "Gabriel", 6 Bd. Gabriel, 21100 Dijon (France)

C. LECOMTE

Laboratoire de Minéralogie-Cristallographie, Equipe de Recherche associée au C.N.R.S., no. 162, Faculté des Sciences, B.P. 239, 54506 Vandoeuvre-les-Nancy Cédex (France)

(Received 23 July 1984)

CONTENTS

A. INTRODUCTION

During the last two decades, the chemistry of metalloporphyrins has been extensively studied and reviewed [1]. However, no review has been devoted solely to titanium and vanadium porphyrins. Fifty years ago, Treibs isolated and identified vanadyl deoxophylloerythroetioporphyrin, the major metalloporphyrin in petroleum and shales [2]. The first synthetic vanadium porphyrin, (*meso*-DME)V=O, was also prepared by Treibs [3], whereas

0010-8545/85/$09.45

(*meso*-DME)Ti=O the first titanium porphyrin was obtained much later by Tsutsui [4].

The poor reactivity of the vanadyl (Por)V=O and titanyl (Por)Ti=O porphyrins explains the very few studies devoted to these two series of metalloporphyrins. The first notable reaction (1976) of titanyl porphyrins was their transformation into peroxoderivatives [5]. More recently, two convenient procedures for the isolation of dihalogeno titanium(IV) and vanadium (IV) porphyrins were described [6,7]. These latter compounds are extremely reactive and can act as precursors to lower valent titanium(III) and vanadium(II) porphyrins.

In this review we first discuss the chemical and structural results regarding the oxo and peroxo derivatives. Later parts deal with the preparation, spectroscopic, and structural data of dihalogeno complexes. Finally, we attempt to show that the dihalogeno derivatives are particularly effective as intermediates for low-valent porphyrins. The rich coordination chemistry of these highly reactive compounds will be described with particular emphasis on reactions with molecular oxygen, elemental sulfur, and selenium. We concentrate especially on structural and spectroscopic data of representative systems of each class.

B. ABBREVIATIONS AND NOMENCLATURE

(i) Abbreviations

Me	methyl
Et	ethyl
Ph	phenyl
mT	*m*-tolyl
pT	*p*-tolyl
AcO	acetate
Acac	acetylacetonate
Cp	cyclopentadienyl
n-Bu_4	n-tetrabutylammonium
1-MeIm	1-methylimidazole
$PPhMe_2$	dimethylphenylphosphine
THF	tetrahydrofuran
NTA	nitrilotriacetate
dipic	dipicolinate
P^{Me}	CH_2–CH_2–$COOCH_3$
p^H	CH_2–CH_2–COOH
$OEPMe_2$	α,γ-Dimethyl-α,γ-dihydrooctaethylporphyrinate
DPEP	deoxophylloerythroetioporphyrinate
Por	unspecified porphyrinate

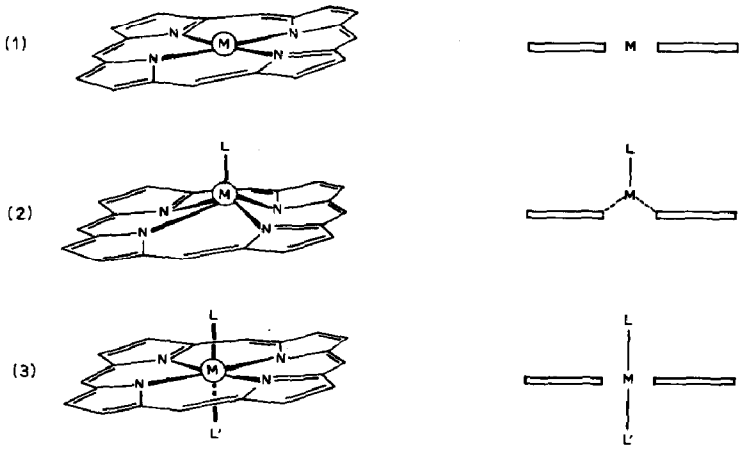

Fig. 1. Usual porphyrin coordination schemes: (1) square planar, (2) square pyramidal, and (3) pseudo-octahedral.

The usual porphyrin coordination schemes are given in Fig. 1.

(ii) Nomenclature

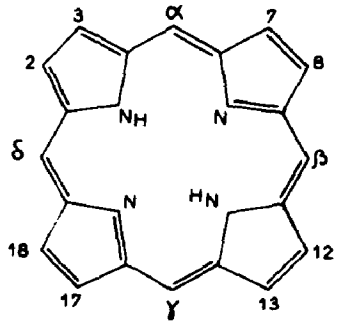

Formula 1

Abbreviation	Name	Substituents								
		2	3	7	8	12	13	17	18	$\alpha,\beta,\gamma,\delta$
P	Porphine	H	H	H	H	H	H	H	H	H
OMP	Octamethylporphyrin	Me	Me	Me	Me	Me	Me	Me	Me	H
OEP	Octaethylporphyrin	Et	Et	Et	Et	Et	Et	Et	Et	H
TPP	Tetraphenylporphyrin	H	H	H	H	H	H	H	H	Ph
TmTP	Tetra-*m*-tolylporphyrin	H	H	H	H	H	H	H	H	mT
TpTP	Tetra-*p*-tolylporphyrin	H	H	H	H	H	H	H	H	pT
Etio-I	Etioporphyrin-I	Me	H	Me	H	Me	P^H	P^H	Me	H
meso-DME	*meso*-Porphyrin-dimethylester	Me	Et	Me	Et	Me	P^{Me}	P^{Me}	Me	H

C. OXO AND PEROXO DERIVATIVES

(i) Titanyl and vanadyl porphyrins: synthesis and characterization

In 1934, Treibs isolated the first oxo vanadium porphyrins and identified the major metalloporphyrin, (DPEP)V=O, in petroleum and shales [2]. Vanadyl porphyrins in fossil plant materials are important as major organic geochemical tracers and provide fundamental information to geochemists [8]. In 1935, the first synthetic vanadium porphyrin (*meso*-DME)V=O was also obtained by Treibs [3]. Petersen [9] later determined the X-ray crystal structure of (DPEP)V=O (Fig. 2) and provided the first crystal data for vanadium porphyrins. In this compound the vanadium–oxygen bond length (1.62(1) Å) is characteristic of the VO^{2+} unit. The metal atom lies 0.48 Å out of the plane of the four nitrogen atoms (0.54 Å from the mean porphinato plane) and the "radius of the central hole" is 2.04 Å. Native titanium porphyrins have not yet been discovered and (*meso*-DME)Ti=O was synthesized only seventeen years ago [4].

Two general methods can be used to prepare titanyl and vanadyl porphyrins: the first uses $(Acac)_2M{=}O$ for metalation in phenol, and the second, MCl_4 or MCl_3 in various solvents. The reaction conditions and references for these two synthetic methods are summarized in Table 1 together with other less common techniques.

Titanyl and vanadyl porphyrins possess M=O stretching vibration frequencies in the range 1050–950 cm^{-1} [4,15,16]. Infrared evidence for the association of vanadium porphyrins in various solvents has been reported

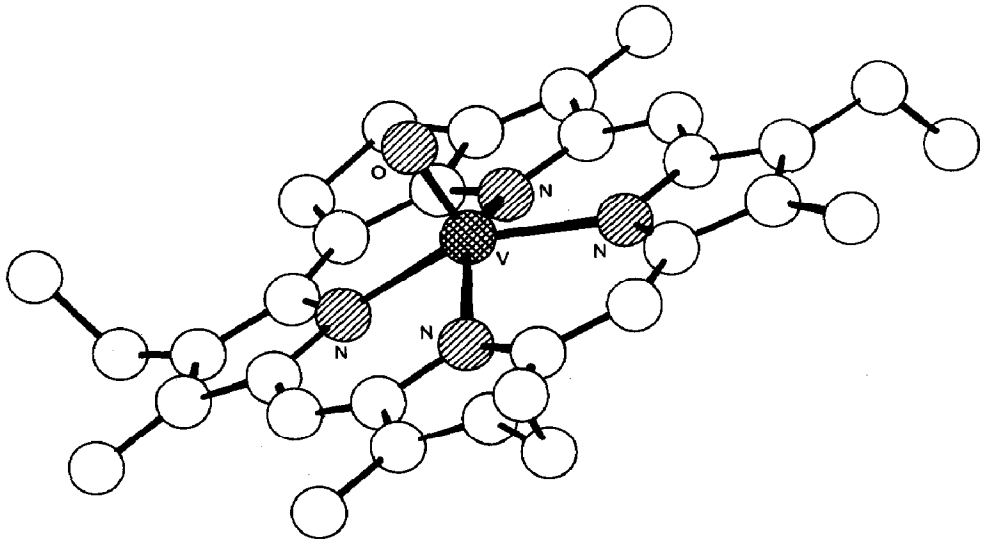

Fig. 2. Crystal structure of (DPEP)V=O.

TABLE 1

Reaction conditions and metalating systems serving to prepare (Por)M=O (M = Ti, V)

Metalating system	Temperature (°C)	Metal inserted	References
$(Acac)_2M=O$/phenol	180–240	Ti, V	10
$(SO_4)V=O$/AcOH	100	V	11, 12
$M(Ph)_2$	200	Ti	4
$M(Cl)_4$		V	3, 12
$M(Cl)_4$/solvent	115–191	Ti	13
$M(Cl)_3$/PhCN	191	V	14

[16]. The electronic spectra of the two series are "normal", consisting of an intense band near 400–420 nm (Soret band) and a group of two (or three) bands between 450 and 650 nm (α and β bands) [17,18]. Coordinating solvents do not modify the electronic spectra of these oxometalloporphyrins [13]. Oxovanadium(IV) porphyrins bound with a crown ether have been synthesized [19]. The cations K^+, Cs^+, NH_4^+, and Ba^{2+}, which require two crown ether cavities for complexation, induce dimerization of the porphyrin. Substituted tetraphenyltitanylporphyrins exhibit non-equivalent phenyl protons due to phenyl ring rotation [20]. ^1H and ^{14}N ENDOR spectra of randomly oriented oxovanadium(IV) tetraphenylphorphyrin have been studied in a frozen solution [21], these techniques furnishing proof of the presence of oxovanadium porphyrins in phosphate mineral extract [22]. Voltammetric studies of the (Por)Ti=O and (Por)V=O complexes show the four waves (two anodic and two cathodic) expected for the macrocycle ring oxidation and reduction reactions [13,23].

The X-ray crystal structures of (OEP)Ti=O [24], (OEP)V=O [25], (TPP)Ti=O [26], (DPEP)V=O [9], and $(OEPMe_2)$Ti=O [27] have been determined. Figure 3 is the ORTEP view of (OEP)Ti=O. The (OEP)V=O and (OEP)Ti=O complexes have also been studied by EXAFS spectroscopy [28,29]. In all these oxo complexes, the metal atom is coordinated by the four nitrogen atoms of the porphyrin ring and a double-bonded oxygen atom. This resulting polyhedron is an almost perfect square pyramid for (OEP)V=O, (OEP)Ti=O, and (TPP)Ti=O. Table 2 gives the stereochemical data of the coordination sphere of the oxo complexes as measured by X-ray diffraction or by EXAFS spectroscopy. The metal–oxygen and metal–nitrogen distances are almost equal for either titanium or vanadium (CM–O = 1.618 ± 0.005 Å; $\langle M-N \rangle = 2.106 \pm 0.008$ Å). Consequently, the out-of-plane distance ($\Delta 4N$) of the metal atom is 0.54 Å, as postulated in 1966 from extended Huckel calculations [30]. Furthermore, Table 2 illustrates the excellent agreement between the X-ray and EXAFS results, showing that EXAFS is a powerful tool for the investigation of the coordination sphere of

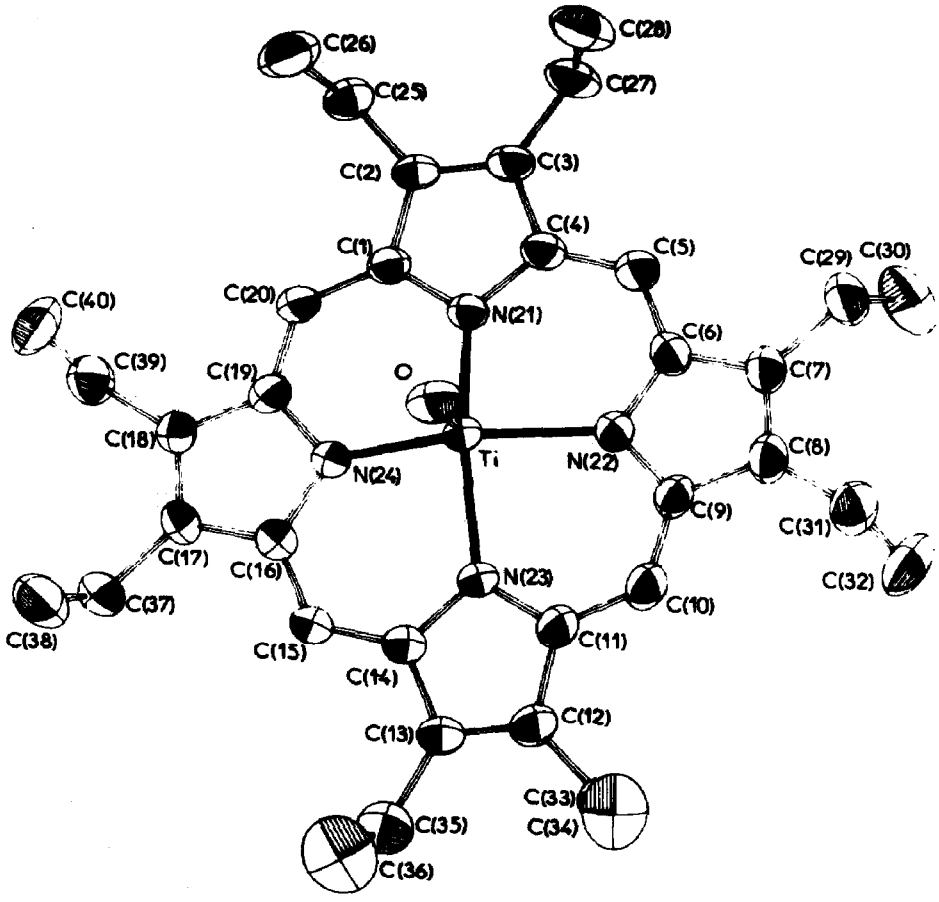

Fig. 3. ORTEP view of (OEP)Ti=O.

metalloporphyrins. This is of value because porphyrins are known often to give crystals of poor quality. The EXAFS method has also been used for probing the structural chemical environment of vanadium in two different

TABLE 2

Stereochemical data of the coordination sphere of some oxo vanadium and titanium porphyrins

Compound	⟨M–N⟩ [a]	M=O [a]	N–C_t [a]	Δ4N [a]	Ref.
(OEP)Ti=O [b]	2.114(5)	1.613(4)	2.040	0.55	24(b)
(OEP)V=O [b]	2.102(3)	1.620(2)	2.029	0.54	25
($OEPMe_2$)Ti=O [b]	2.110(3)	1.619(4)	2.030	0.58	27
(DPEP)V=O [b]	2.10(1) [d]	1.62(1)	2.04	0.48	9
(OEP)V=O [c]	2.08 ± 0.02	1.61 ± 0.01			28
(DPEP)V=O [c]	2.10 [d]	1.61			28
(TPP)Ti=O [c]	2.11 ± 0.02	1.64 ± 0.05			29

[a] Values given in Å. [b] X-ray diffraction data. [c] EXAFS data. [d] Average value calculated on the three unsubstituted pyrrole rings; the other V–N value is 1.96 Å.

fractions of a Boscan asphaltene [28]: the V–N distances found agree well with those found by X-ray crystallography (Table 2). Furthermore, this study led to the conclusion that vanadylporphyrins are the dominant components of vanadium compounds in these asphaltenes.

(ii) Peroxo titanium(IV) porphyrins

Little work has been devoted to the chemistry of titanyl and vanadyl porphyrins because of the inertness and the unusually high bond energy of the MO^{2+} unit. The first notable reaction was the attack of benzoyl peroxide or hydrogen peroxide on oxotitanium(IV) porphyrins leading to the corresponding peroxo derivatives (Por)Ti(O_2) [5], the first metalloporphyrin with a dioxygen moiety bonded "side-on" to the metal (Scheme 1).

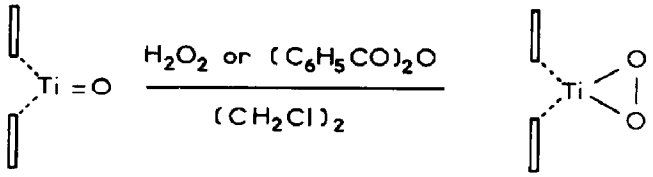

Scheme 1

The peroxidic nature of these complexes was proven on the basis of spectrochemical and crystallographic data. The (Por)Ti(O_2) compounds exhibit three IR absorption bands near to 890, 650, and 600 cm^{-1} and by analogy with other peroxotitanium(IV) complexes [31–33], the higher frequency band is assigned to the O–O stretching, and the other two bands to symmetric and asymmetric M–O stretch modes (Fig. 4).

The crystal structure of (OEP)Ti(O_2) is given in Fig. 5 [5,24(b)]. The complex is isotypic to the monoclinic forms of (OEP)Ti=O [24(b)] and (OEP)V=O [25]. In the peroxo complex, the coordination polyhedron of the titanium atom is reduced to C_{2v}, the metal being hexacoordinated by the four nitrogen atoms of the porphyrin and by two oxygen atoms symmetrically bonded on the same side of the porphyrin (Ti–O(1) = 1.827(4), Ti–O(2) = 1.822(4) Å). The O(1)–O(2) distance (1.445(5) Å) is characteristic of a peroxo moiety. These bond lengths are similar to those found in other peroxotitanium compounds (Table 3). The titanium atom lies 0.620(6) Å from the plane of the four nitrogen atoms and 0.657(6) Å from the mean plane of the macrocycle, compared to 0.555(6) and 0.609(6) Å for (OEP)Ti=O (Fig. 6). The radius of the central hole of the porphyrin is reduced to 2.016 Å, being 2.040 Å in (OEP)Ti=O. Contrary to (OEP)Ti=O the titanium–nitrogen bond lengths are not equivalent: the mean value of the Ti–N(22) and Ti–N(24) distances is 2.128(4) ± 0.005 Å and the corresponding value

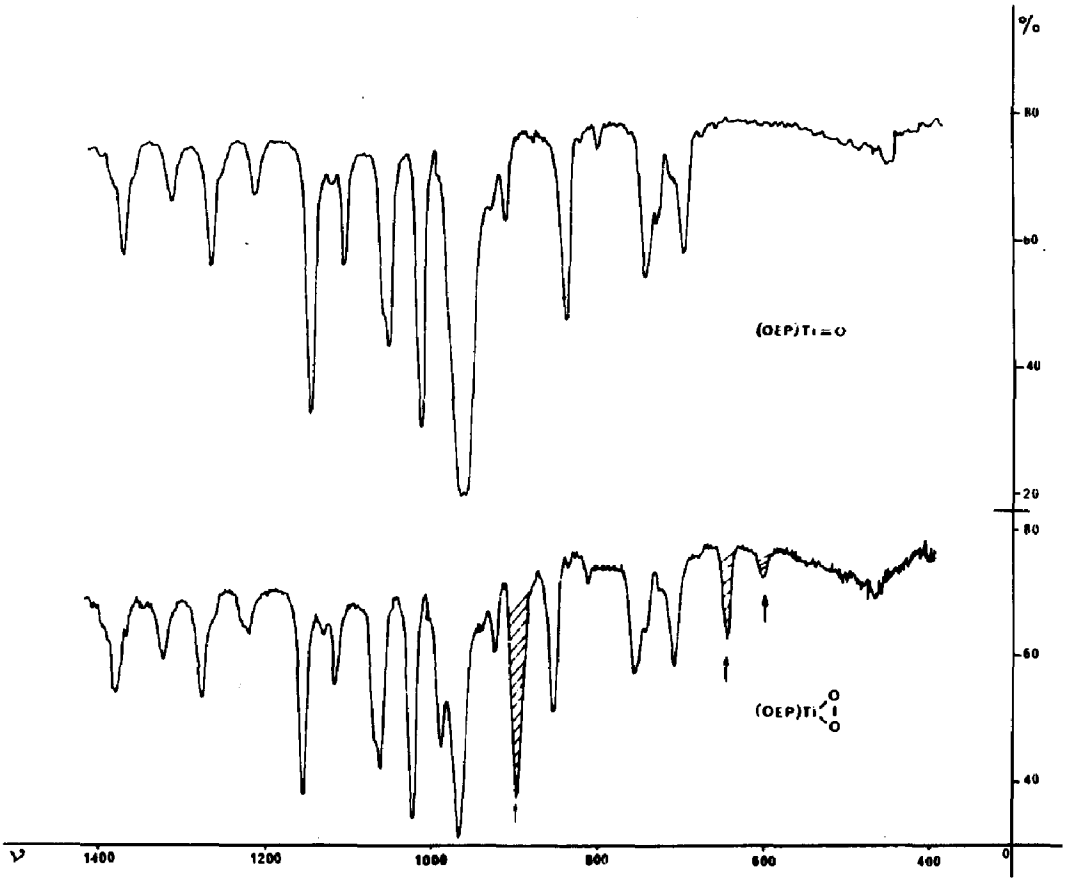

Fig. 4. IR spectra of (OEP)Ti=O and (OEP)Ti(O_2).

for the other two Ti–N bonds is 2.090(4) ± 0.004 Å. This significant difference is explained by the specific positions of the peroxide group which eclipses almost perfectly the N(22)–N(24) nitrogen atoms. This particular conformation has also been found in (TpTP)Mo(O_2)$_2$ [39].

^{1}H and ^{13}C dynamic NMR data on (OEP)Ti(O_2) and (TPP)Ti(O_2) show them to be fluxional. Down to about −50°C the peroxo ligand undergoes fast exchange between two equivalent sites, when the peroxo group eclipses the two equivalent pairs of opposite nitrogen atoms. The barrier to rotation of the peroxo group at the coalescence temperature is 10.8 ± 0.5 kcal mol^{-1} (Tc = −50°C) for (TPP)Ti(O_2) and 9.9 ± 0.5 kcal mol^{-1} (Tc = −65°C) for (OEP)Ti(O_2) [24(b)]. These dynamic NMR measurements show that this preferred conformation exists in solution as well as in the solid state and thus is not imposed by crystal packing constraints. Furthermore, ab initio calculations relative to an unsubstituted (P)Ti(O_2) complex are in very good agreement with all the experimental observations: a side-on conformation is found to be more stable than the bent end-on structure by 83 kcal mol^{-1}

TABLE 3

Crystallographic data for some titanium(IV) peroxo complexes

Complex	Ti–O(1)	Ti–O(2)	O(1)–O(2)	Ti–O(1)–O(2)	O(1)–O(2)–Ti	O(1)–Ti–O(2)	Ref.
$[H_2O(dipic)Ti(O_2)]_2O$	1.872(7)	1.905(7)	1.45(1)			45.2(4)	34
$(H_2O)_2(dipic)Ti(O_2)$	1.834(2)	1.858(2)	1.464(2)	67.50(6)	67.78(6)	46.72(6)	35
triclinic	1.842(1)	1.862(1)	1.469(1)				36
$(H_2O)_2(dipic)Ti(O_2)$	1.833(1)		1.458(2)	66.56(2)		46.88(6)	37
orthorhombic	1.844		1.477				36
$[F_2(dipic)Ti(O_2)]^{2-}$	1.846(4)	1.861(4)	1.463(5)	67.3(2)	66.2(2)	46.5(2)	35
$\{[(NTA)Ti(O_2)]_2O\}^{4-}$	1.892(2)	1.889(2)	1.469(2)	67.02(6)	67.26(6)	45.72(6)	38
	1.897	1.898	1.481				
$(OEP)Ti(O_2)$	1.827(4)	1.822(4)	1.445(5)	66.5(2)	66.9(2)	46.7(2)	5, 24(b)

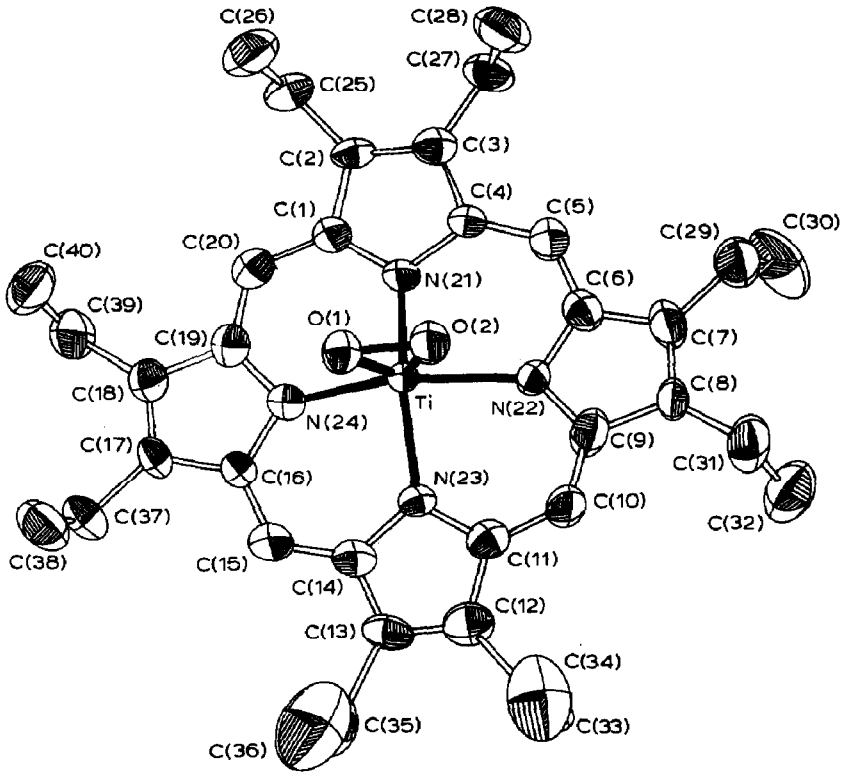

Fig. 5. ORTEP view of (OPE)Ti(O_2).

[40,41], the stability being due to the metal dioxygen interaction $3d_{xz}$–π_g^a. Furthermore, the eclipsed configuration of the peroxo group is the result of a titanium–dioxygen interaction $3d_{xy}$–π_g^b (Fig. 7), which cannot occur in the

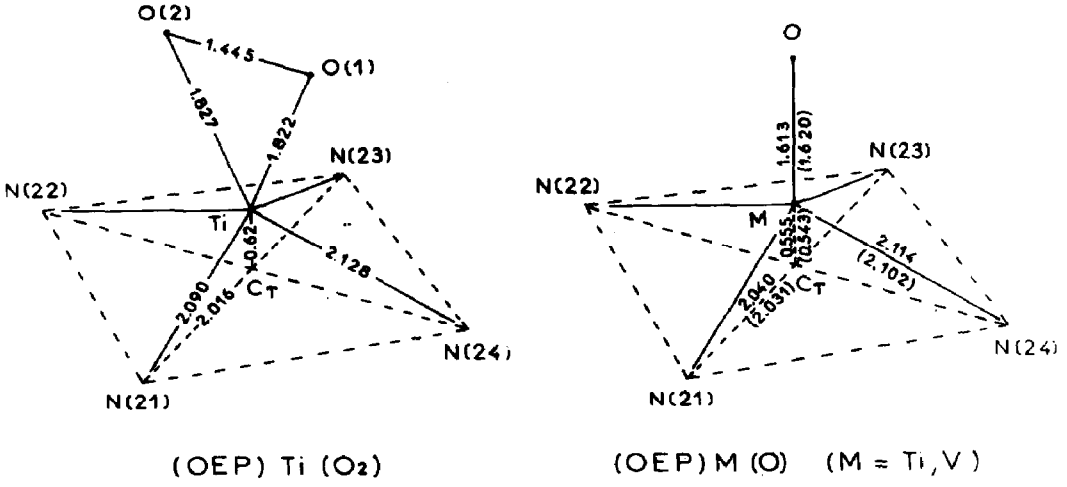

Fig. 6. Schematic views of the coordination of the metal in (OEP)Ti(O_2), (OEP)Ti=O, and (OEP)V=O (values between brackets refer to (OEP)V=O).

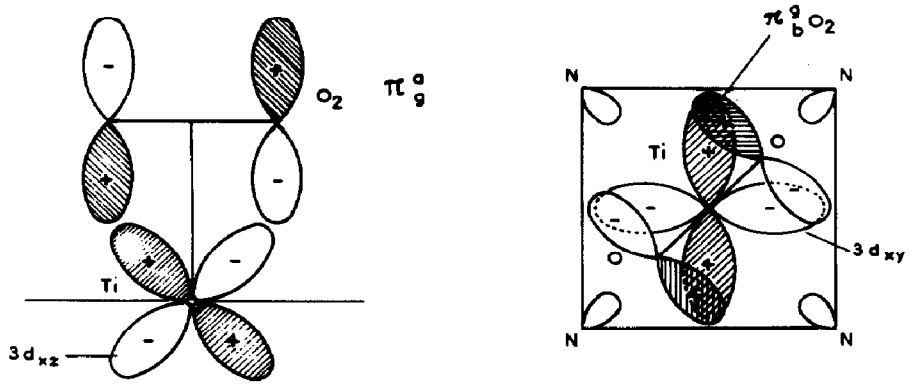

Fig. 7. Bonding scheme of the TiO_2 unit.

staggered conformation because the $d_{x^2-y^2}$ level is too high. This conclusion was also proposed by other authors from qualitative considerations [42,43].

The cyclic voltammetry curve of (Por)Ti(O_2) exhibits the four one-electron waves (two anodic and two cathodic) expected for the ring oxidation and reduction reactions [24(b)]. An additional reduction step in a two-electron irreversible process is observed ($E_{1/2} \simeq -1$ V) just before the first ring reduction waves. This additional reduction occurs at the axial peroxide ligand with resulting cleavage of the O–O bond to generate two oxide ions, one of which is coordinated to the Ti(IV) ion.

These peroxo compounds are related to those of cobalt: some cobalt peroxide complexes can be obtained either by oxidative addition of dioxygen to a low valent metal complex, or by ligand exchange on a high valent complex [44] (Scheme 2). Formally, the peroxo complexes of titanium(IV) porphyrins are identical to the oxidative addition products of dioxygen on the hypothetical titanium(II) porphyrins [45].

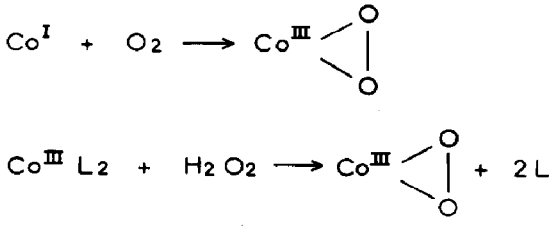

Scheme 2

D. DIHALOGENO DERIVATIVES

(i) Titanium(IV) complexes

The action of the hydrogen halides HX (X = F, Cl, Br) on oxotitanium(IV) porphyrins leads to the dihalogeno complexes (Por)Ti($X)_2$ [6], (Por)Ti($F)_2$

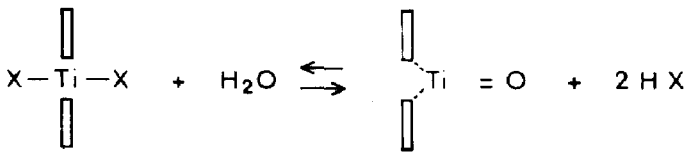

Scheme 3

being the first complex isolated [6(a)] via a reversible process (Scheme 3) [6(b)]. Far infrared spectra show the expected bands for titanium terminal halogen stretching vibrations (ν(Ti–F) = 647, ν(Ti–Cl) = 358, and ν(Ti–Br) = 280 cm^{-1}). The (TPP)Ti$(Br)_2$ complex (Fig. 8 [46]) crystallizes in the tetragonal space group *I4/m* with the titanium on the inversion center. The resulting symmetry of the coordination polyhedron (C_{4h}) is imposed by the space group: the titanium atom is octahedrally coordinated by the four nitrogen atoms and two bromide ions and lies in the perfect porphyrin plane. The radius of the central hole measured here by the Ti–N distance (2.062(8) Å) is longer than that found in (OEP)Ti(O_2) (2.016(6) Å) and in (OEP)Ti=O

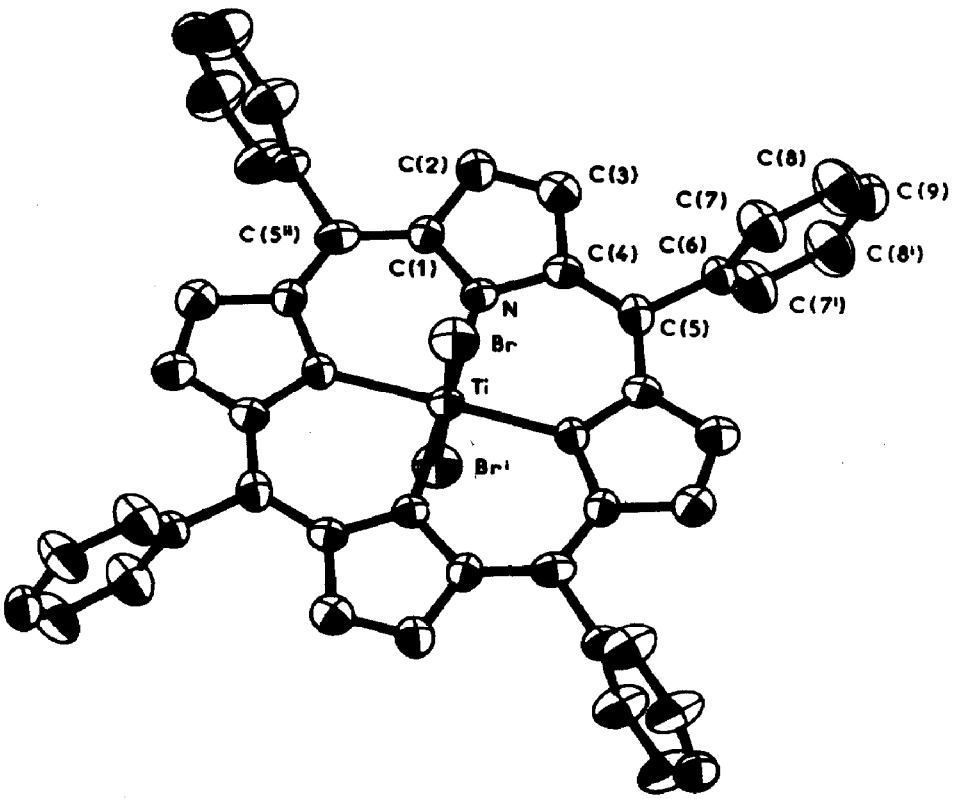

Fig. 8. ORTEP view of (TPP)Ti$(Br)_2$ [46].

(2.040(6) Å). This crystal structure gave the first Ti(IV)–Br bond length (2.454(2) Å) for a coordination compound.

(ii) Vanadium(IV) complexes

Contrary to titanyl porphyrins, the vanadyl complexes (Por)V=O do not react with hydrogen halides: the deoxygenation of (Por)V=O however, can be obtained by the action of SOX_2 or $(COX)_2$ under mild conditions to yield the dihalogeno vanadium(IV) complexes (Scheme 4) [7]. This method can be used also to prepare dihalogeno titanium complexes [47]. Gaseous HBr bubbled through a solution of $(Por)V(Cl)_2$ affords $(Por)V(Br)_2$. The expected bands for the vanadium–halogen stretching vibrations are given in Table 4 together with the corresponding ones in the titanium series. EXAFS at the bromine K edge of $(OEP)V(Br)_2$ [7] allows discrimination between the two possible *trans* or *cis* configurations. Figure 9 gives the corrected pseudo-radial distributions $\chi_1(R)$ and $\chi_2(R)$ including the phase shift corrections for the Br*–V shell and the Br*–N shell respectively. The interatomic distances Br–V, 2.41 Å (Fig. 9(a)) and Br–N, 3.18 Å (Fig. 9(b)) agree well with those of $(TPP)Ti(Br)_2$ (see above). Furthermore, the intensity of the

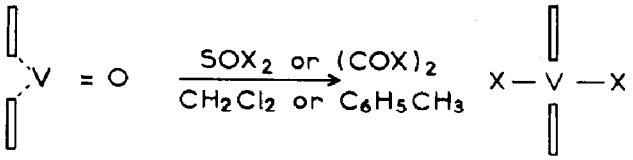

Scheme 4

TABLE 4

Characteristic IR bands of $(Por)V(X)_2$ [7] and $(Por)Ti(X)_2$ [6(b),48]

Complex [a]	ν(V–X) cm^{-1}	ν(Ti–X) cm^{-1}
$(OEP)M(F)_2$	–	620
$(OEP)M(Cl)_2$	335	330
$(OEP)M(Br)_2$	250	240
$(TPP)M(F)_2$	–	647
$(TPP)M(Cl)_2$	355	358
$(TPP)M(Br)_2$	285	280
$(TmTP)M(Cl)_2$	345	–
$(TmTP)M(Br)_2$	270	–
$(TpTP)M(Cl)_2$	350	–
$(TpTP)M(Br)_2$	280	–

[a] M = V, Ti.

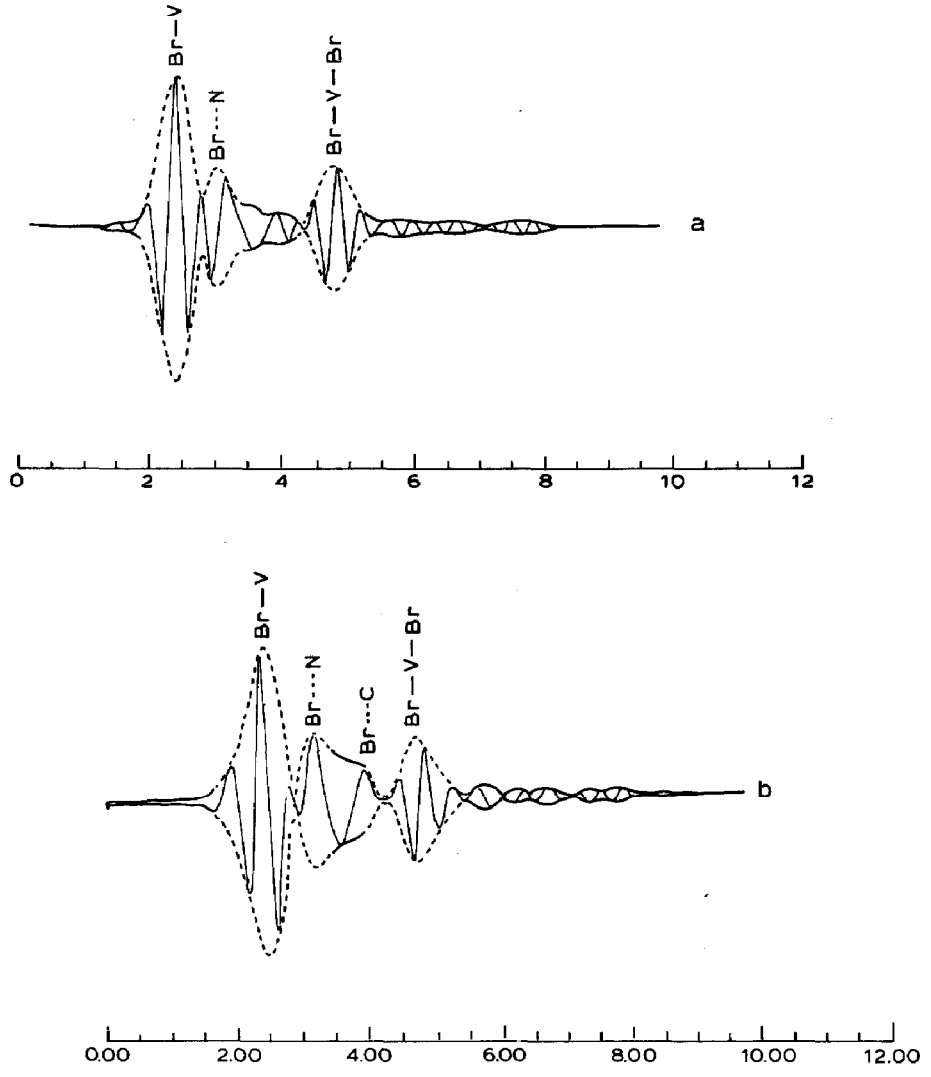

Fig. 9. EXAFS pseudo-radial distribution $\tilde{\chi}(R)$ of $(OEP)V(Br)_2$ bromine K edge. (a) Phase-shift corrections are for the Br* · · · V shell ($E_0 = 13468$ eV). (b) Phase-shift corrections are for the Br* · · · N shell ($E_0 = 13474.0$ eV).

signal at ca. 4.85 Å suggests the linear Br–V–Br sequence and provides strong evidence for an undistorted *trans* configuration (focusing effect).

High resolution ^1H NMR spectra of $(Por)V(X)_2$ exhibit the broad lines expected for a paramagnetic porphyrin complex (signal between 1 and 21 ppm), although no EPR spectrum was found even at 77 K. INDO/S calculations [7], performed on a dichloro vanadium(IV) unsubstituted porphyrin $(Por)V(Cl)_2$, suggest that the lowest occupied orbital corresponds to a doubly degenerate E_g state, and explains the lack of an EPR signal.

E. LOW VALENT PORPHYRINS

(i) Titanium series

Reduction of the (Por)Ti(X)$_2$ complexes with zinc amalgam gives monohalogenotitanium(III) complexes (Por)Ti(X) [49,51]. The characteristic IR stretching modes of Ti–X of the tetraphenyl derivatives (TPP)Ti(X), and the EPR data are given in Table 5. Changes in the EPR and UV–visible spectra upon addition of ligands are explained by the formation of six-coordinated complexes, while electrochemical or chemical (sodium anthracenide) reduction can lead to anionic species such as (TPP)Ti(F)$_2^-$.

The reactivity of (TPP)Ti(F) with various aryl Grignard reagents [50], alkyl and aryl thiolates [51], and molecular oxygen has been studied [49]. The metal aryl-bonded complexes (TPP)Ti(Ar) have been prepared by the aryl Grignard reagents (Scheme 5). These aryl compounds exhibit a nine-line EPR spectrum similar to that of (TPP)Ti(F). Contrary to (TPP)Ti(F), addition of various ligands (toluene, *N*-methylimidazole, THF) to (TPP)Ti(Ar) does not modify the UV–visible and EPR spectra corresponding to the former species. These observations can be correlated to the difference between the relative electrodonor properties of aryl and fluoride ligands.

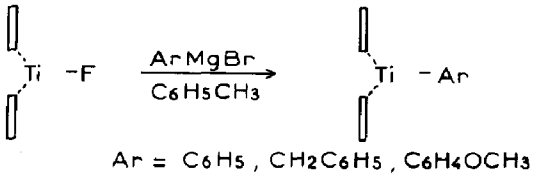

Scheme 5

TABLE 5

EPR and IR data of various halogeno titanium porphyrins [48,49]

Complex	IR		EPR		
	ν(Ti–X) (cm^{-1})	g	a_N/G	a_F/G	a_L/G
(TPP)Ti(F)	680	1.972	2.29	11.1	
[(TPP)Ti(F)$_2$](n-Bu$_4$)	535	1.968	2.20	6.7	2.7(F)
(TPP)Ti(F)(THF)	620	1.965	2.35	9.6	
(TPP)Ti(F)(1-MeIm)	595	1.961	2.5	9.8	1.0(N), 0.7(N)
(TPP)Ti(Cl)	440	1.964			
(TPP)Ti(Br)	345	1.976			
(TPP)Ti(I)		1.974	2.25		

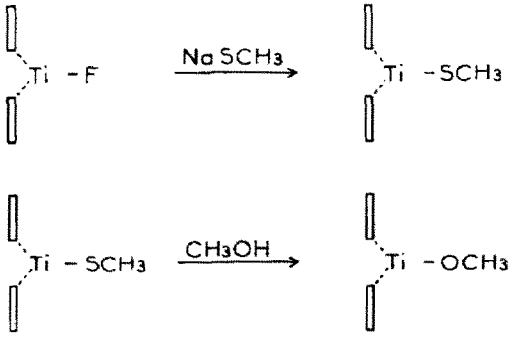

Scheme 6

Benzenethiolatotitanium(III) tetraphenylporphyrin (TPP)Ti(SC_6H_5) was obtained by adding sodiumbenzenethiolate to (TPP)Ti(F). Preferential five coordination of (TPP)Ti(SC_6H_5) is observed similar to the σ-bonded titanium–carbon series. Methoxotitanium(III) tetraphenylporphyrin (TPP)Ti(OCH_3) results from the axial ligand substitution of (TPP)Ti(SCH_3) by reaction of methanol with (TPP)Ti(SCH_3) [52] (Scheme 6). The titanium(III)–nitrogen distances (2.12(2) Å) in (TPP)Ti(OCH_3) (Fig. 10) are

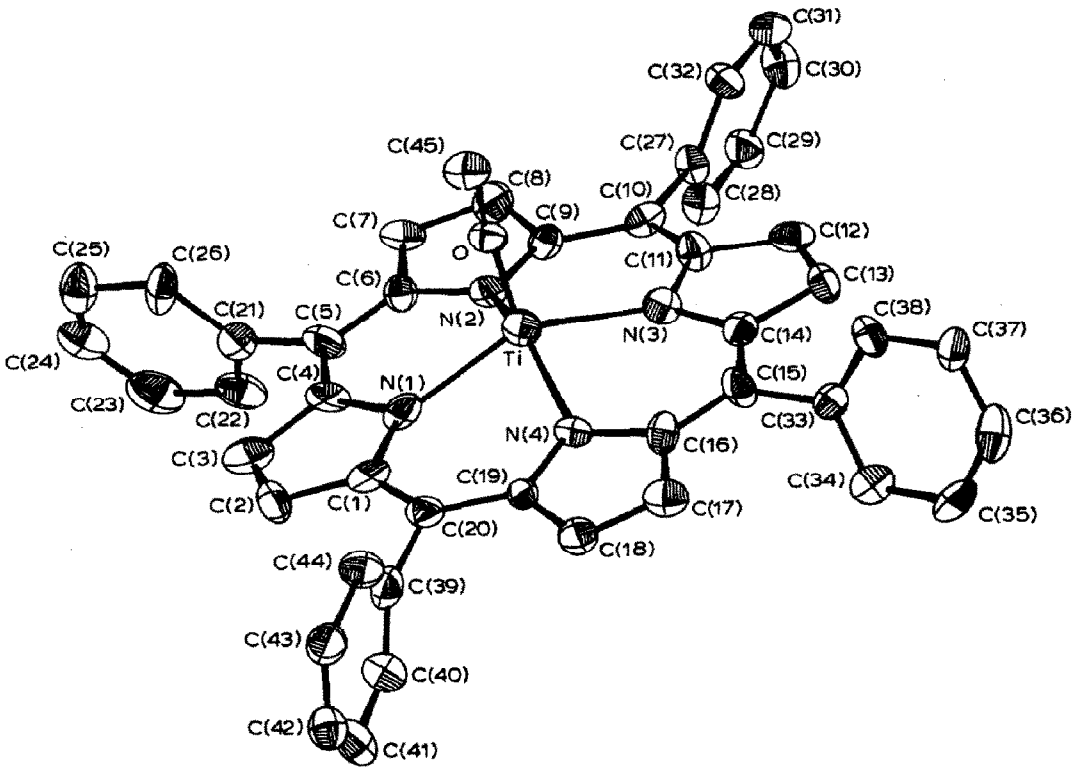

Fig. 10. ORTEP view of (TPP)Ti(OCH_3) [52].

TABLE 6

Stereochemical data for the coordination polyhedron of methoxo metalloporphyrins.

Complex	Distances		M–O–C	Δ4N [a]	Ref.
	M–N	M–O			
(TPP)Ti(OCH_3)	2.12(2)	1.77(1)	171 (1)	0.62(2)	52
(TPP)Fe(OCH_3)	2.082(2)	1.815(1)	129.1(1)	0.484(1)	53
(*meso*-DME)Fe(OCH_3)	2.073(6)	1.842(4)	125.9(6)	0.455	54
(TPP)Co(OCH_3)(Py)	1.96(1)	1.92(4)	121 (4)	0.0	55
(P)Ge(OCH_3)$_2$ [b]	2.015(4)	1.821(3)	124.0(3)	0.0	56
	2.015(4)	1.822(3)	123.9(3)	0.0	

[a] Δ4N is the distance of the metal from the plane of the four nitrogen atoms. [b] Two half molecules in the asymmetric unit of the crystal.

close to those found in titanium(IV) porphyrins. Consequently the titanium(III) atom lies 0.62 Å out of the plane of the four nitrogen atoms. Table 6 shows that the methoxo ligand deviates significantly from the bent geometry (Ti–O–C = 171(1)°) and that the titanium–oxygen bond length is short (Ti–O = 1.77(1) Å) compared with the iron [53,54], cobalt [55], or germanium [56] methoxoporphyrins. These results correlate with the decrease in number of valence electrons of the metals, and suggest an increasing π-donation from the oxygen atom, leading to a shorter titanium–oxygen bond.

The exposure of (TPP)Ti(F) to molecular oxygen gives a mixture of roughly equal amounts of *trans* (TPP)Ti(F)$_2$ and (TPP)Ti(O_2) [49] (Scheme 7). A superoxide intermediate (TPP)Ti(O_2)(F) is postulated for this reaction, since such an intermediate has been detected in a solid state EPR study [49]. In the case of (TPP)Ti(Ar) (Ar = C_6H_5, SC_6H_5), autoxidation generates (TPP)Ti=O and Ar–Ar products (Scheme 8)

(ii) Vanadium series

On the basis of extended Hückel calculations, low valent vanadium(II) porphyrins have been predicted [57], and indeed reduction of dihalogenovanadium(IV) porphyrins directly produces the corresponding

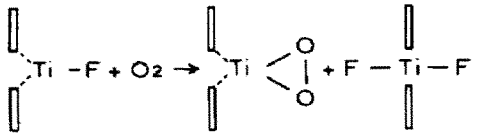

Scheme 7

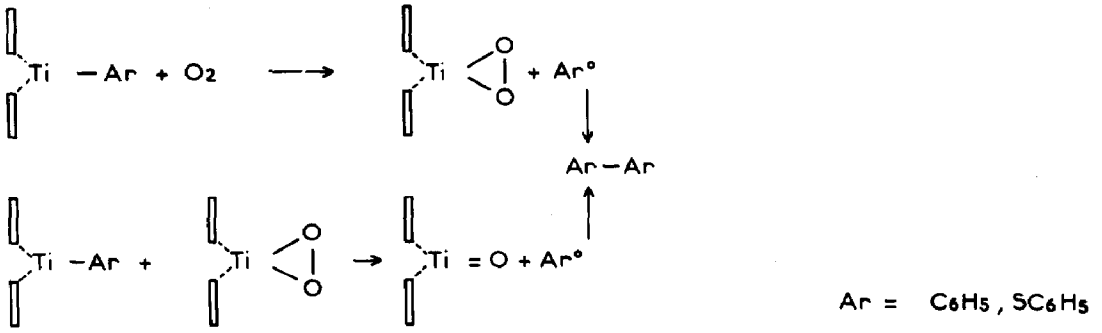

Scheme 8

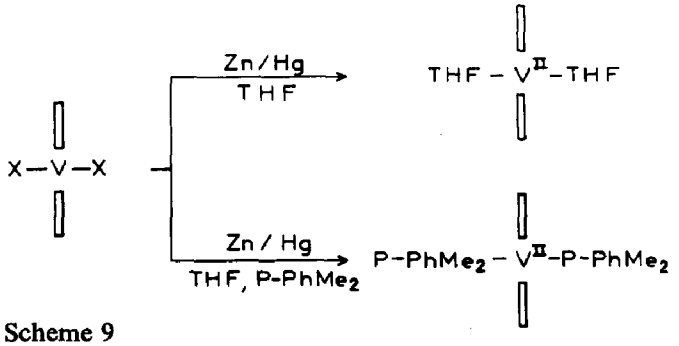

Scheme 9

vanadium(II) complexes *trans*-(Por)V(L)$_2$ (L = THF, PPhMe$_2$; Por = OEP, TPP, TpTP, TmTP) [58,59] (see Scheme 9).

Electronic spectra of (Por)V(L)$_2$ are typical of hyperporphyrinic systems, the intensities of bands I and II being of the same magnitude [60]. The magnetic moment of (OEP)V(PPhMe$_2$)$_2$ (μ_{eff} = 3.52 BM) is consistent with a d^3 complex, although no EPR signal is found for this kind of compound because spin–orbit coupling might occur.

Figures 11 and 12 give the ORTEP views of (OEP)V(THF)$_2$ and (OEP)V(PPhMe$_2$)$_2$. In the two (Por)V(L)$_2$ molecules, the vanadium is at an inversion center, lies in the perfect plane of the four nitrogen atoms and is octahedrally coordinated. The symmetry is almost D_{4h} in (OEP)V(THF)$_2$ (N(1)–V–O: 89.2(1); N(2)–V–O: 89.9(2)°), whereas in (OEP)V(PPhMe$_2$)$_2$ (N(1)–V–P: 92.0(1); N(2)–V–P: 87.7(1)°) the slight distortion could be due to crystal packing. The mean V–N distances are statistically equivalent (2.051(4) in (OEP)V(PPhMe$_2$)$_2$ and 2.046(4) in (OEP)V(THF)$_2$), and are comparable with the metal–N distances observed in (*meso*-tetraphenylporphyrinato)bis[bis(diphenylphosphino)methane]ruthenium(II) (2.041(8) Å) [61] and in (*meso*-tetraphenylporphyrinato)bis(tetrahydrofuran)iron(II) (2.057(2) Å) [62,63]. As expected for a d^3 ion, the V–N distances are slightly greater (0.02 Å) than the mean distance Ct $\cdots$ N (2.031(2) Å) observed in

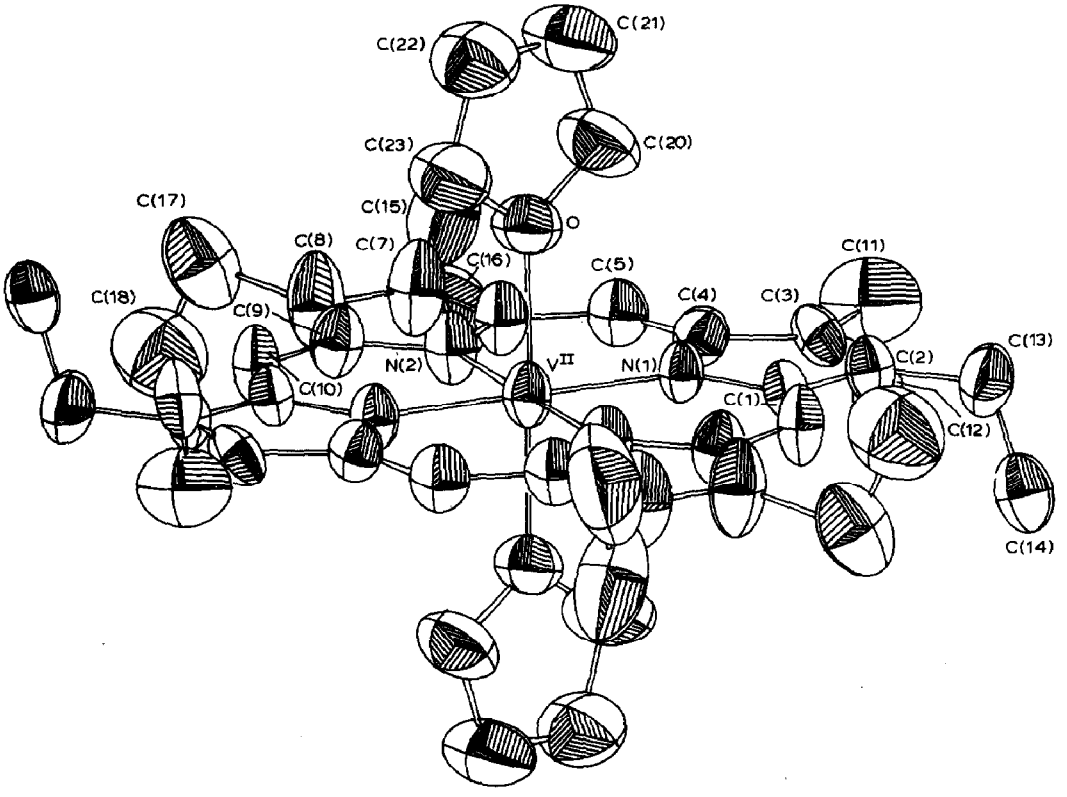

Fig. 11. ORTEP view of $(OEP)V(THF)_2$ [59].

(octaethylporphyrinato)oxovanadium(IV) [25] and characterize a small expansion of the porphyrinic core (Ct is the center of the macrocycle).

In $(OEP)V(THF)_2$ the axial bond length V–O (2.174(4) Å) is much shorter than that observed in $(TPP)Fe(THF)_2$ (Fe–O: 2.351(3) Å at room temperature [62] and 2.288(1) at 100 K [63]), this resulting from occupancy of the d_{z^2} orbital in the high spin ferrous complex ($S = 2$).

In $(OEP)V(PPhMe_2)_2$ the vanadium–phosphorus distance (2.523(1) Å), the first example of a vanadium(II)–phosphorus bond length, is slightly longer than those observed in vanadium(0) phosphine complexes (2.442(2) Å in *cis*$[\eta^5\text{-}C_5H_5V(CO)_2(Ph_2PCH_2CH_2PPh_2)]$ [64] and 2.360(2) Å in $[(CO)_4V(PMe_2)]_2$ [65]).

Convenient procedures for the isolation of thio- and seleno–vanadium(IV) porphyrins have been reported [66,67]. The action of vanadium(II) porphyrins with elemental sulfur leads to (Por)V=S (Scheme 10); in contrast low valent organometallic compounds usually react with elemental sulfur to give pentasulfide molecules [68,69,70]. The (Por)V=Se complex is prepared simply by substituting the more soluble complex $(cyclopentadienyl)_2TiSe_5$ for elemental selenium.

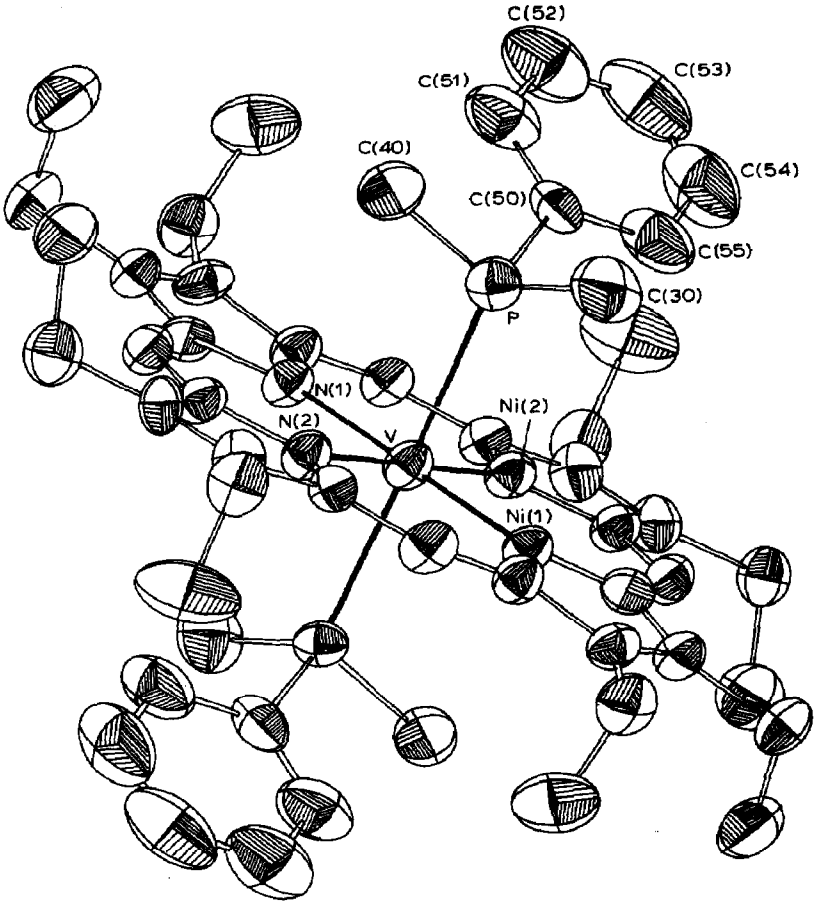

Fig. 12. ORTEP view of (OEP)V($PPhMe_2$)$_2$ [58,59].

The IR spectra of the thio- and seleno-vanadium porphyrins exhibit a medium to strong intensity band in the 550–565 cm^{-1} (V=S) and 434–447 cm^{-1} (V=Se) ranges, respectively, these stretching frequencies being anoma-

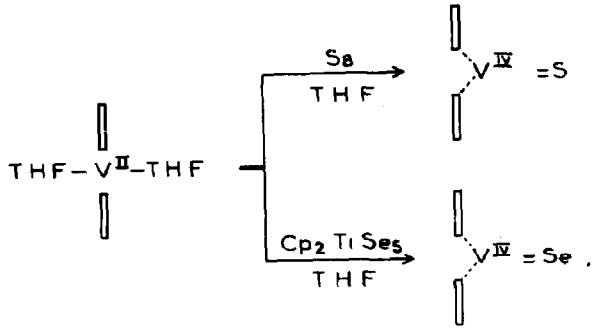

Scheme 10

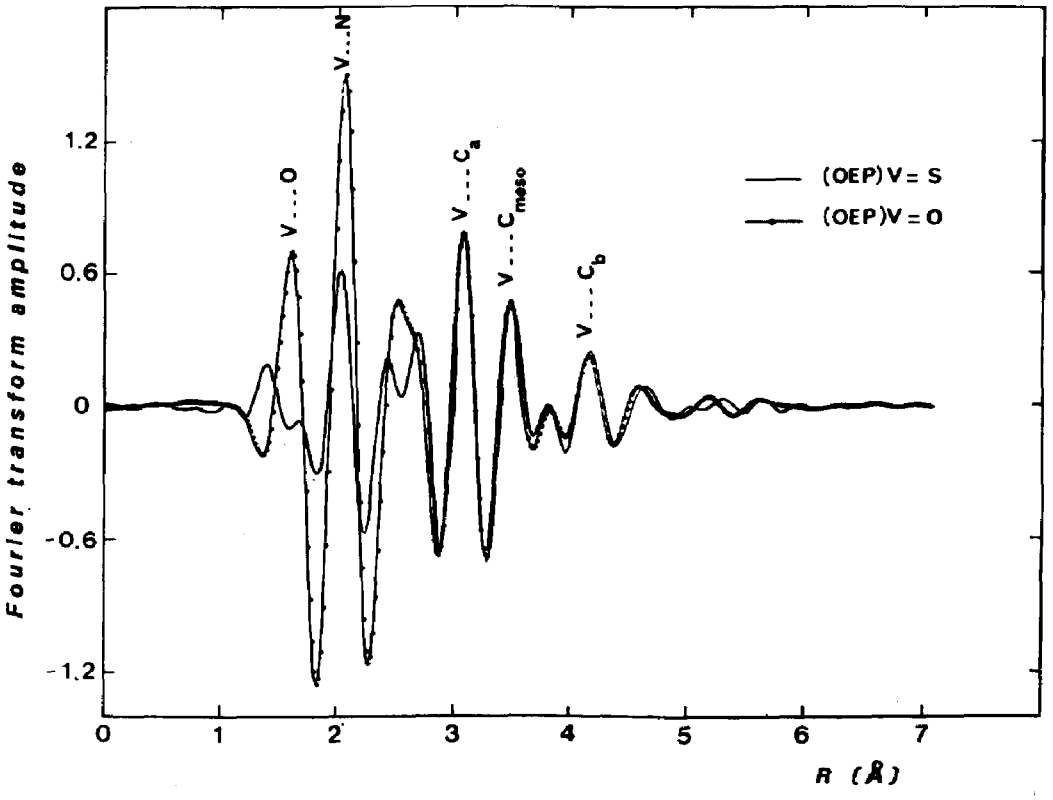

Fig. 13. Comparison of the imaginary part of the Fourier transformed spectra $I_m\tilde{\chi}(R)$ of (OEP)V=O and (OEP)V=S.

lously low compared with that of V=O ($\simeq 1000\ cm^{-1}$). The same observation is made for some oxo and thio vanadium–Schiff base complexes [71]. As observed for vanadium(II) porphyrins, UV–visible spectra of thio– and seleno–vanadium(IV) porphyrins are typical of hyperporphyrins [60].

EXAFS data of (OEP)V=O, (OEP)V=S, and (OEP)V=Se have been recorded at the K edges of vanadium and selenium [(OEP)V=Se] [66,67,72]. For the sake of comparison, Figs. 13 and 14 show the magnitude of the Fourier transform spectra and the imaginary part $I_m\tilde{\chi}(R)$ of both systems (OEP)V=O and (OEP)V=S and (OEP)V=O and (OEP)V=Se obtained at the vanadium K edge. As illustrated, the contribution of the C_α, C_m, C_β carbons is fairly identical for the three systems, whereas strong distortions affect the V · · · N and V · · · S(Se) signals. This has been explained by a scattering phase shift difference between S and N for (OEP)V=S. As the geometry of the porphyrinic core remains identical (Figs. 13 and 14), difference Fourier transform spectra have been computed for both systems: (OEP)V=O minus (OEP)V=S and (OEP)V=O minus (OEP)V=Se. As shown in Fig. 15, a nearly perfect cancellation of the EXAFS signals of the porphyrin macrocycle is

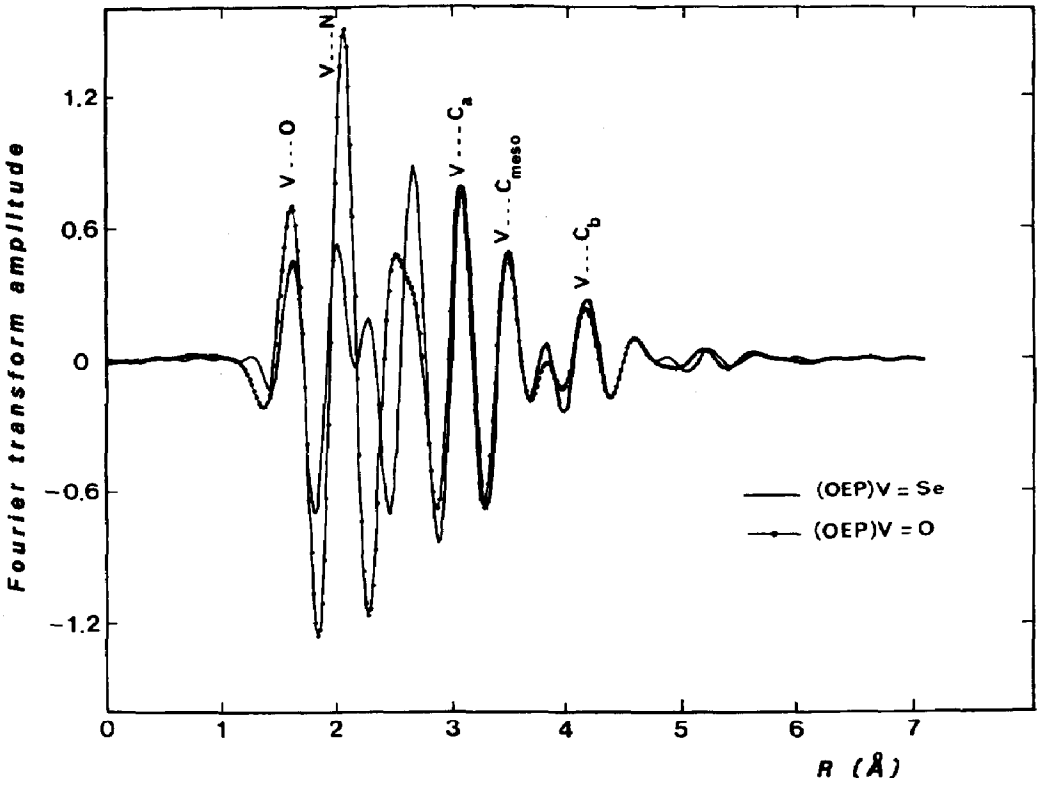

Fig. 14. Comparison of the imaginary part of the Fourier transformed spectra $I_m\tilde{\chi}(R)$ of (OEP)V=O and (OEP)V=Se.

observed for both difference spectra. In the case of (OEP)V=S, the difference Fourier spectrum exhibits a negative contribution of the V=O shell ($R_1 = 1.61 \pm 0.02$ Å) with the expected V=S signal ($R_2 = 2.06 \pm 0.02$ Å), the phase

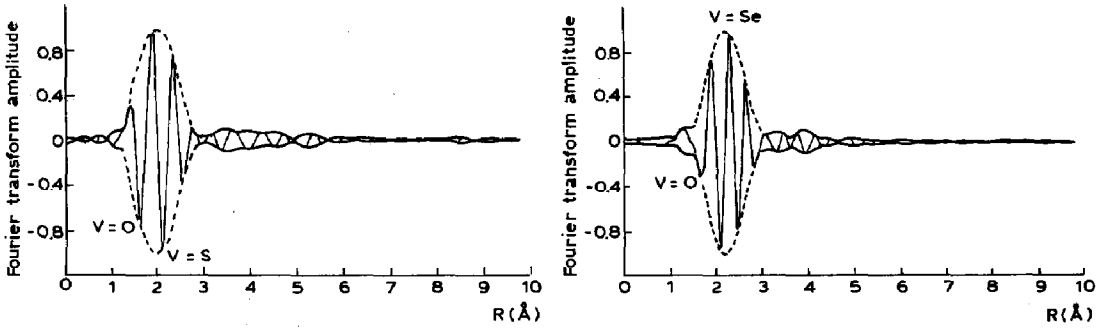

Fig. 15. Difference Fourier spectra: dotted line: $|\tilde{\chi}(R)|$; full line: $I_m\tilde{\chi}(R)$. (a) (OEP)V=S minus (OEP)V=O. (b) (OEP)V=S minus (OEP)V=O.

TABLE 7

EPR data of (Por)V=Y complexes (Y = S, Se, or O)

Complex	g_{iso}	$g^{\parallel}$	$g^{\perp}$	$A_{iso} \times 10^4$ (cm^{-1})	$A^{\parallel} \times 10^4$ (cm^{-1})	$A^{\perp} \times 10^4$ (cm^{-1})
(OEP)V=S	1.969	1.964	1.972	−79.8	−143.4	−51.5
(TPP)V=S	1.971	1.965	1.971	−80.3	−142.1	−50.9
(TmTP)V=S	1.973	1.965	1.973	−80.5	−144.1	−51.0
(TpTP)V=S	1.973	1.966	1.972	−80.7	−141.5	−51.8
(OEP)V=Se	1.956	1.970	1.944	−79.2	−136.1	−51.4
(TPP)V=Se	1.957	1.971	1.946	−80.1	−135.6	−53.0
(TmTP)V=Se	1.956	1.971	1.948	−80.0	−136.8	−53.3
(TpTP)V=Se	1.956	1.971	1.947	−79.7	−136.6	−53.6
(OEP)V=O	1.979	1.962	1.985	−88.7	−158.7	−56.5
(TPP)V=O	1.979	1.964	1.985	−89.3	−158.3	−55.6
(TmTP)V=O	1.978	1.962	1.984	−89.6	−159.0	−56.5
(TpTP)V=O	1.979	1.964	1.986	−89.0	−159.4	−56.3

$g^{\parallel} = g_e - (8\xi\delta^2\alpha^2/\Delta^{\parallel})$, $g^{\perp} = g_e - (2\xi\delta^2\gamma^2/\Delta^{\perp})$ with $g_e = 2.0023$; α, β, γ being defined in ref. 73; $\Delta^{\parallel} = (E(b_1) - E(b_2))$; $\Delta^{\perp} = (E(e) - E(b_2))$; ξ = spin–orbit coupling constant. $\Delta^{\parallel} = -K + P[-(4/7)\delta^2 + (g^{\parallel} - g_e) + (3/7)(g^{\perp} - g_e)]$ and $\Delta^{\perp} = -K + P[(2/7)\delta^2 + (11/14)(g^{\perp} - g_e)]$, with K Fermi isotropic coupling term, and $P = g_e\beta_e g_N\beta_N\langle r^{-3}\rangle$ (r: radial extension of $3d$ orbital).

of the latter being clearly negative. For (OEP)V=Se, the difference spectrum is dominated by the expected positive signal of the V=Se shell ($R_2 = 2.19 \pm 0.03$ Å). The latter result is confirmed by the EXAFS data at the selenium K edge (R_1(Se* · · · V) = 2.185 ± 0.02 Å). Furthermore, from these results it was possible to estimate the out-of-plane distance ($\Delta 4N = 0.47 \pm 0.04$ Å).

The room temperature and frozen solution EPR data of the (Por)V=S and (Por)V=Se complexes are given in Table 7 [67], together with corresponding values for (Por)V=O. The observed parameters are characteristic of a d^1 V(IV) nucleus.

The reduced energy splittings deduced from the EPR data are given in Table 8.

The observed values of $g_{\perp}$ and $\Delta^{\perp}/\gamma^2$ are in good agreement with the electronegativity of the three elements O > S > Se; thus, the metal–ligand bond energy decreases in the same order. The parameter $g_{\parallel}$ which strictly depends on the metal–macrocycle porphyrin interaction increases from the oxo to the seleno series. These observations correlate with the out-of-plane distance found by EXAFS for (OEP)V=Se (0.47 Å) compared to 0.57 Å in (OEP)V=O.

TABLE 8

Calculated values of $\Delta^{\parallel}/\alpha^2$, $\Delta^{\perp}/\gamma^2$, P, and K for (Port)V=S, (Por)V=Se, and (Por)V=O

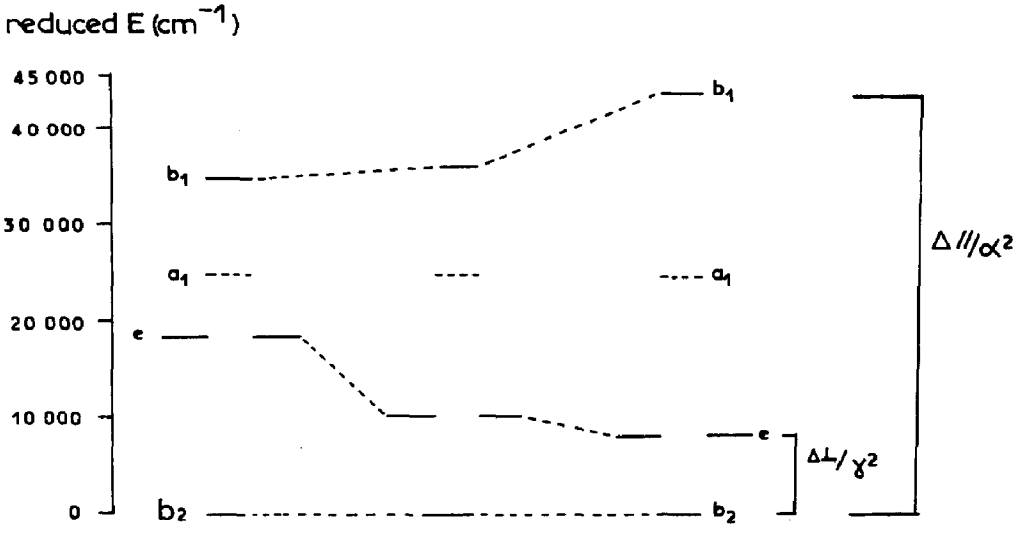

Complex	$\Delta^{\parallel}/\alpha^2$ (cm^{-1})	$\Delta^{\perp}/\gamma^2$ (cm^{-1})	$P \times 10^4$ (cm^{-1})	$K \times 10^4$ (cm^{-1})
(OEP)V=S	35190	10940	103.8	78.7
(TPP)V=S	37870	10700	103.3	77.9
(TmTP)V=S	37200	11550	105.4	78.7
(TpTP)V=S	37310	11180	101.6	78.4
(OEP)V=Se	42560	5710	97.6	74.8
(TPP)V=Se	44340	5960	95.3	76.0
(TmTP)V=Se	44120	6080	96.1	76.6
(TpTP)V=Se	43790	6080	95.6	76.8
(OEP)V=O	34070	19690	114.7	87.7
(TPP)V=O	35410	19450	115.4	87.0
(TmTP)V=O	33620	17990	115.0	87.7
(TpTP)V=O	35520	20300	115.9	87.9

F. CONCLUSION

Because of their wide distribution in nature, almost all the work devoted to the vanadium porphyrins concerns the geochemistry of these compounds and the synthesis of model derivatives which could occur during the chemical processing of oils and shales. More specifically, low valent vanadium porphyrins have been studied and characterized.

The most important result in the field of titanium porphyrins has been the synthesis of the first peroxo metalloporphyrin. These systems have initiated a lot of research for this family of complexes; two recent papers give some new results: in the former the electrochemistry of oxo and peroxo titanium is studied and the ECEC mechanism of the electron reduction of the peroxoligand is described [74]. In the second it has been shown that (TPP)Ti=O is a catalyst for the epoxidation of olefins by alkyl-hydroperoxides; an intermediate *cis* hydroxo alkylperoxo complex is proposed as the active species [75].

The structural characterization of some representative derivatives of these two series has been made by X-ray diffraction techniques and EXAFS spectroscopy. For (OEP)V=O and (OEP)Ti=O, the two techniques led to the same metal ligand distances (M=O, ⟨M–N⟩) showing that EXAFS is a powerful tool for probing the coordination scheme in metalloporphyrins.

REFERENCES

1 (a) K.M. Smith (Ed.), Porphyrins and Metalloporphyrins, Elsevier, Amsterdam, 1975.
(b) D. Dolphin (Ed.), The Porphyrins, Vols. I–VII, Academic Press, New York, 1979.
(c) A.B.P. Lever and H.B. Gray, Iron Porphyrins, Parts 1 and 2, Addison–Wesley, Reading, MA, 1983.
2 (a) A. Treibs, Justus Leibigs Ann. Chem., 510 (1934) 42.
(b) A. Treibs, Angew. Chem., 49 (1936) 682.
3 A. Treibs, Justus Leibigs Ann. Chem., 517 (1935) 172.
4 M. Tsutsui, R.A. Velapoldi, K. Suzuki, and T. Koyano, Angew. Chem., 80 (1968) 914.
5 R. Guilard, M. Fontesse, P. Fournari, C. Lecomte, and J. Protas, J. Chem. Soc., Chem. Commun., (1976) 161.
6 (a) J.W. Buchler in D. Dolphin (Ed.), The Porphyrins, Vol. IA, Academic Press, New York, 1979, 435.
(b) M. Nakajima, J.M. Latour, and J.C. Marchon, J. Chem. Soc., Chem. Commun., (1977) 763.
7 P. Richard, J.L. Poncet, J.M. Barbe, R. Guilard, J. Goulon, D. Rinaldi, A. Cartier, and P. Tola, J. Chem. Soc., Dalton Trans., (1982) 1451.
8 E.W. Baker and S.E. Palmer in D. Dolphin (Ed.), The Porphyrins, Vol. IA, Academic Press, New York, 1979.
9 R.C. Pettersen, Acta Crystallogr. Sect. B, 25 (1969) 2527.
10 J.W. Buchler, G. Eikelmann, L. Puppe, K. Rohbock, H.H. Schneehage, and D.D. Weck, Justus Leibigs Ann. Chem., 745 (1971) 135.
11 R. Bonnett and P. Brewer, Tetrahedron Lett. (1970) 2579.
12 J.G. Erdman, V.G. Ramsey, N.W. Kalenda, and W.E. Hanson, J. Am. Chem. Soc., 78 (1956) 5844.
13 P. Fournari, R. Guilard, M. Fontesse, J.M. Latour, and J.C. Marchon, J. Organomet. Chem., 110 (1976) 205.
14 J.M. Barbe and R. Guilard, unpublished results.
15 M. Tsutsui, R.A. Velapoldi, K. Suzuki, F. Wohwinkel, M. Ichikawa, and T. Koyano, J. Am. Chem. Soc., 91 (1969) 6262.
16 F.E. Dickson and L. Petrakis, J. Phys. Chem., 74 (1970) 2850.

17 M. Gouterman, L.K. Hanson, G.E. Khalil, J.W. Buchler, K. Rohbock, and D. Dolphin, J. Am. Chem. Soc., 97 (1975) 3142.
18 K. Ueno and A.E. Martell, J. Phys. Chem., 60 (1956) 934.
19 V. Thanabal and V. Krishnan, Inorg. Chem., 21 (1982) 3606.
20 A.L.W. Schroyer, C. Lorberau, S.S. Eaton, and G.R. Eaton, J. Org. Chem., 45 (1980) 4296.
21 C.F. Mulks and H.V. Willingen, J. Phys. Chem., 85 (1981) 1220.
22 H.V. Willingen, C.F. Mulks, A. Bouhaouss, M. Fehrat, and A.H. Roufosse, J. Am. Chem. Soc., 102 (1980) 4846.
23 (a) J.H. Fuhrhop, Tetrahedron Lett., 37 (1969) 3205.
(b) J.H. Fuhrhop, K.M. Kadish, and D.G. Davis, J. Am. Chem. Soc., 95 (1973) 5140.
24 (a) C. Lecomte, J. Protas, and R. Guilard, C.R. Acad. Sci., Ser. C, 281 (1975) 921.
(b) R. Guilard, J.M. Latour, C. Lecomte, J.C. Marchon, J. Protas, and D. Ripoll, Inorg. Chem., 17 (1978) 1228.
25 F.S. Molinaro and J.A. Ibers, Inorg. Chem., 15 (1976) 2278.
26 C. Riche, private communication.
27 P.N. Dwyer, L. Puppe, J.W. Buchler, and W.R. Scheidt, Inorg. Chem., 14 (1975) 1782.
28 J. Goulon, A. Retournard, P. Friand, C. Goulon-Ginet, C. Berthe, J.F. Müller, J.F. Poncet, R. Guilard, J.C. Escalier, and B. Neff, J. Chem. Soc., Dalton Trans., (1984) 1095.
29 J. Goulon, P. Friant, J.L. Poncet, R. Guilard, J. Fischer, and L. Ricard, in A. Bianconi, L. Incoccia, and S. Stipcich (Eds.), EXAFS and Near Edge Structure, Springer Series in Chemical Physics, 27 (1983) 100.
30 M. Zerner, and M. Gouterman, Inorg. Chem., 5 (1966) 1699.
31 W.P. Griffith, J. Chem. Soc., (1964) 5248.
32 E. Wendling, Bull. Soc. Chim. Fr., (1967) 16.
33 J. Mühlebach, K. Müller, and D. Schwarzenbach, Inorg. Chem., 9 (1970) 2381.
34 D. Schwarzenbach, Inorg. Chem., 9 (1970) 2391.
35 D. Schwarzenbach, Helv. Chim. Acta, 55 (1972) 2990.
36 D. Schwarzenbach, Z. Kristallogr., Kristallgeom., Kristallphys., Kristallchem., 143 (1976) 429.
37 H. Manohar and D. Schwarzenbach, Helv. Chim. Acta, 57 (1974) 1086.
38 D. Schwarzenbach and K. Girgis, Helv. Chim. Acta, 58 (1975) 239.
39 B. Chevrier, T. Diebold, and R. Weiss, Inorg. Chim. Acta, 19 (1976) L57.
40 M.M. Rohmer, M. Barry, A. Dedieu, and A. Veillard, Int. J. Quantum Chem., Quantum Biol. Symp., 4 (1977) 337.
41 A. Dedieu, M.M. Rohmer, H. Veillard, and A. Veillard, Nouv. J. Chim., 3 (1979) 653.
42 C. Lecomte, Thesis of "Doctorat d'Etat" Nancy, France (1979).
43 Y. Ellinger, J.M. Latour, J.C. Marchon, and R. Subra, Inorg. Chem., 7 (1978) 2025.
44 B. Bosnich, H. Boucher, and C. Marshall, Inorg. Chem., 15 (1976) 634.
45 C.J. Boreham, J.M. Latour, J.C. Marchon, B. Boisselier, P. Cocolios, and R. Guilard, Inorg. Chim. Acta, 45 (1980) L69.
46 C. Lecomte, J. Protas, J.C. Marchon, and M. Nakajima, Acta Crystallogr. Sect. B, 34 (1978) 2858.
47 J.M. Barbe, and R. Guilard, unpublished results.
48 J.M. Latour, Thesis of "Doctorat d'Etat" Grenoble, France (1980).
49 J.M. Latour, J.C. Marchon, and M. Nakajima, J. Am. Chem. Soc., 101 (1979), 3974.
50 J.M. Latour, C.J. Boreham, and J.C. Marchon, J. Organomet. Chem., 190 (1980) C61.
51 J.C. Marchon, J.M. Latour, and C.J. Boreham, J. Mol. Catal., 7 (1980) 227.
52 C.J. Boreham, G. Buisson, E. Duée, J. Jordanov, J.M. Latour, and J.C. Marchon, Inorg. Chim. Acta, 70 (1983) 77.

53 C. Lecomte, D.L. Chadwick, P. Coppens, and E.D. Stevens, Inorg. Chem., 22 (1983) 2982.
54 J.L. Hoard, M.H. Hamor, T.A. Hamor,, and W.D. Caughey, J. Am. Chem. Soc., 87 (1965) 2312.
55 C. Riche, A. Chiaroni, M. Perrée-Fauvet, and A. Gaudemer, Acta Crystallogr. Sect. B, 34 (1978) 1868.
56 A. Mavridis and A. Tulinski, Inorg. Chem., 15 (1976) 2723.
57 M. Zerner and M. Gouterman, Inorg. Chem., 5 (1966) 1699.
58 J.L. Poncet, J.M. Barbe, R. Guilard, H. Oumous, C. Lecomte, and J. Protas, J. Chem. Soc., Chem. Commun., (1982) 1421.
59 H. Oumous, C. Lecomte, J. Protas, J.L. Poncet, J.M. Barbe, and R. Guilard, J. Chem. Soc., Dalton Trans., (1984) 2677.
60 M. Gouterman, in D. Dolphin (Ed.), The Porphyrins, Vol. III, Academic Press, New York, 1978, p. 1.
61 R.G. Bahl, G. Domazetis, D. Dolphin, B.R. James, and J. Trotter, Inorg. Chem., 20 (1981) 1556.
62 C.A. Reed, T. Mashiko, W.R. Scheidt, K. Spatalian, and G. Lang, J. Am. Chem. Soc., 102 (1980) 2302.
63 C. Lecomte, P. Coppens, R.H. Blessing and L. Li, XIII International Congress of Crystallography, Hamburg FRG, 1984, Collected Abstracts C-168.
64 D. Rehder, I. Müller, and J. Kopf, Inorg. Nucl. Chem., 40 (1978) 1013.
65 H. Vahrenkamp, Chem. Ber., 111 (1978) 3472.
66 J.L. Poncet, R. Guilard, P. Friant, and J. Goulon, Polyhedron, 5 (1983) 417.
67 J.L. Poncet, R. Guilard, P. Friant, C. Goulon-Ginet, and J. Goulon, Nouv. J. Chim., 8 (1984) 583.
68 A.P. Ginsberg, W.E. Lindsell, C.R. Spinkle, K.W. West, and R.L. Cohen, Inorg. Chem., 21 (1982) 3666.
69 S. Gambarotta, C. Floriani, A. Chesi-Villa, and N.C. Guastini, J. Chem. Soc., Chem. Commun., (1983) 184.
70 G. Muller, J.L. Petersen, and N.L.F. Dahl, J. Organomet. Chem., 111 (1976) 91.
71 K.P. Callahan and P.J. Durand, Inorg. Chem., 19 (1980) 3211.
72 J. Goulon, C. Goulon-Ginet, P. Friant, J.L. Poncet, R. Guilard, J.P. Battioni, and D. Mansuy, Proceedings of the Fourth International Conference on the Organic Chemistry of Selenium and Tellurium, 1983, 379.
73 W.C. Lin, in D. Dolphin (Ed.), The Porphyrins, Vol. IV, Academic Press, New York, 1979, 355.
74 T. Malinski, D. Chang, J.M. Latour, J.C. Marchon, M. Gross, A. Giraudeau, and K. Kadish, Inorg. Chem., 23 (1984) 3947.
75 H.J. Ledon and F. Varescon, Inorg. Chem., 23 (1984) 2735..
76 P. Friant, J. Goulon, J. Fischer, L. Ricard, M. Schappacher, R. Weiss, and J. Momenteau, Nouv. J. Chim., 9 (1985) 33.